Light-in-flight holographic PIV (LiFH-PIV) for wind-tunnel applications: Off-site reconstruction of deep-volume real particle images

Sven F. Herrmann* and Klaus D. Hinsch

Keywords: HPIV, particle hoplography, light-in-flight holography (LiFH), Nd:YAG laser (pulsed/cw), noise limit, wind tunnel, 3D flow measurement

Abstract

Holographic particle imaging techniques for air flow investigations are mainly limited to small scale laboratory experiments. The two main reasons are a) the limited light power available in conjunction with small tracer-particle sizes, which must be in the order of one micron to properly probe air flows, and b) increased background noise from out-of-focus particles in deep volumes preventing investigations with higher particle densities. To ensure a good accuracy of the velocity measurements by faithful reconstruction geometry, the evaluation of particle images is often conducted in the original recording setup. The time-consuming scanning process, however, blocks the flow facility during evaluation - a disadvantage for measurements in costly industrial wind tunnels. For an alternative, we have introduced off-site reconstruction and evaluation. In recent papers (Hinrichs et al. 1997, Herrmann and Hinsch 2001) we have furthermore demonstrated principles to cope with little object light and suppress background noise. Here we present a successful implementation of theses principles for wind tunnel measurements.

Introduction

Particle holography is the most promising technique to map the three-dimensional velocity distribution of complex non-stationary flows (Hinsch 2002). Such measurements are truly instantaneous and non-invasive. But air-flows, and especially those of high complexity, are yet difficult to investigate with holographic particle image velocimetry (HPIV) - the extension of PIV to the third dimension. For this technique two holograms are recorded from a flow seeded with tracer particles. During reconstruction their respective particle images are compared to determine a three dimensional displacement and the local velocity is calculated. Researchers are concerned with a couple of problems, from which those most essential for wind-tunnel measurements are reviewed in this section. The basics of solutions to cope with weak object light and noise are recalled, and an application to wind-tunnel measurements is described.

1.1 Weak object light

The holographic recording of particles within air flows has been demonstrated many times in laboratory-scale experiments. But since µm-size particles have to be introduced to faithfully

* Applied Optics Group, Faculty V, Institute for Physics, Carl von Ossietzky University, D-26111 Oldenburg – Germany
phone: +49 (0) 441 798 –3477, fax: -3576, email: herrmann@uni-oldenburg.de

follow the flow, the available light, even from state-of-the-art laser systems, sets limits to the maximum cross-section of the illuminating beam and thus limits the size of the volume which can be investigated. The illuminating beam (object beam) has to be expanded in both dimensions perpendicular to its propagation direction in order to illuminate a deep volume. Typically energy-densities are lowered by one or two orders of magnitude, as compared to PIV where a light sheet is used. The small particles are weak scattering objects, the amount of light scattered can be calculated from Mie-theory (Bohren and Huffmann 1983) and is strongly dependent on particle size. In figure 1 (left) the total scattering cross-section of non-absorbing particles (DEHS, n = 1,453) at a wavelength of $\lambda = 532$ nm is shown versus the particle radius. While for particle radii above 1 μm the corresponding value is mainly determined by the geometrical cross-section of the particle, it is lowered by approximately two orders of magnitude, when the particle radius decreases by one order of magnitude towards 100 nm. Furthermore, intensity variations with scattering angle have to be taken into account for the planning of a setup and the type of particles to be used. In figure 1 (right) the situation for vertically polarized light and for the same DEHS-particles is illustrated. Strong modulations, especially from particles with smaller radii, can prevent from a proper registration under a given angle.

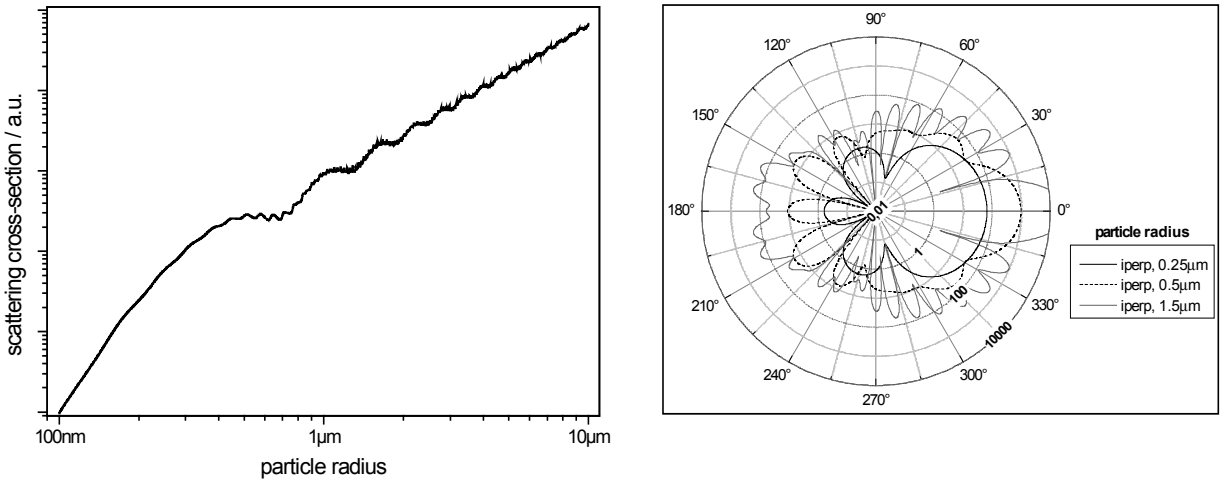

Fig. 1. Total scattering cross-section according Mie-theory of spherical non-absorbing particles (DEHS, n = 1,453) versus particle radius at a wavelength of $\lambda = 532$ nm (left) and the scattering characteristics of such particles when illuminated with vertically polarized light of the same wavelength (right).

The established and yet unsurpassed recording materials for the holograms are still silver halide emulsions (Bjelkhagen 1995). Though these are of low photographic speed, they offer a solution to the weak object light problem. Due to their large dynamic range even weak objects, which do not show up in a reconstructed image under typical conditions, are registered as small transmittance modulations on the film. In the reconstruction these low intensity particle images thus can be detected by integrating light over time on an appropriate sensor. This method has been used in the present study to allow for the proper small seeding particles to investigate a wind tunnel flow and yet allow an extended volume.

1.2 Noise in particle images

Often the relevant flow structures are in the sub-millimeter range, while they have to be recorded simultaneously over a volume of typically several centimeters in size in all dimensions. This

requires dense seeding to sample the field with sufficient accuracy and leads to higher background noise from out-of-focus images. To guarantee a given signal-to-noise ratio the number density of the seeding particles must not exceed a maximum value which grows with the imaging aperture and decreases with the depth of the recorded volume (Pu et al. 2002). Thus, there are two possibilities to properly record such flows:

(1) The aperture may be increased which, however, usually goes with an increasing complexity of the setup (Zhang et al. 1997) or confronts with a variety of unwanted effects related to the recording materials (e.g. emulsion shrinkage and mechanical stability of the substrate) and the optics involved (Barnhart et al. 1994). Such setups are thus unsuitable for wind-tunnel measurements, were industrial needs require practically manageable equipment.

(2) The effective depth must be reduced. This can be achieved even without decreasing the overall depth of the measurement volume by utilizing coherence requirements of holography, resulting in a setup which has been called light-in-flight holography (LiFH) in other context (Abramson 1996). For flow investigations this technique was introduced recently (Hinrichs et al. 1997). An increase in effective signal-to-noise ratio or, accordingly, a higher maximum number density of particles are thus possible.

As long as weak objects are recorded and reconstructed with the integrating method, another source of noise plays an important role. Scattered light from the emulsion grains of the developed holographic plate adds coherently to the out-of-focus noise and can even hide particle images. It can be found that the signal-to-noise ratio of particle images also depends on the ratio between object- and reference intensity during the recording of the hologram (Goodman 1967, Kozma 1968). Yet it is possible to record particle ensembles with object intensities of approximately three orders of magnitude less than necessary to obtain the best diffraction efficiency from a hologram (Herrmann and Hinsch 2001).

1.3 Light in flight holography for flow analysis

Let us briefly recall the use of light sources with a coherence length of only a few millimeters for applications in flow investigations (LiFH-PIV) The idea is the following: object-wave and reference-wave can interfere only when the difference in path these wave have traveled is less than the coherence length of the light. As shown in the example of figure 2, reference light incident from the left has to travel a longer path to the right side of the holographic plate than to the left. Object light scattered from particles is recorded only if this path-length differs by no more than the coherence length L from that of the corresponding reference light. Thus, with proper alignment, particles from a shell in the middle of the observed field are recorded in a small region in the middle of the plate, particles from a front shell on the left and from a rear shell on the right. For the reconstruction of a real image a conjugate reference wave (i.e. inversely traveling wave) is needed to illuminate the hologram. This can be achieved with a single planar wave for recording and reconstruction, when the hologram is turned by 180 degrees after development. Upon reconstruction through a small aperture only a shell with a depth of roughly half a coherence length shows up. The background of holographic particle images is therefore reduced considerably. This method has been applied successfully for the investigation of flows in a small wind tunnel (Hinrichs et al. 1998) and in the transition region of a free air jet (Geiger et al. 2000). These experiments have been performed with a double-pulsed ruby laser – a light source of high energy, yet of many disadvantages. To record separable fields for the removal of

directional ambiguity and for cross-correlation analysis, for example, an electro-optical switch had to be introduced to split the double-pulse.

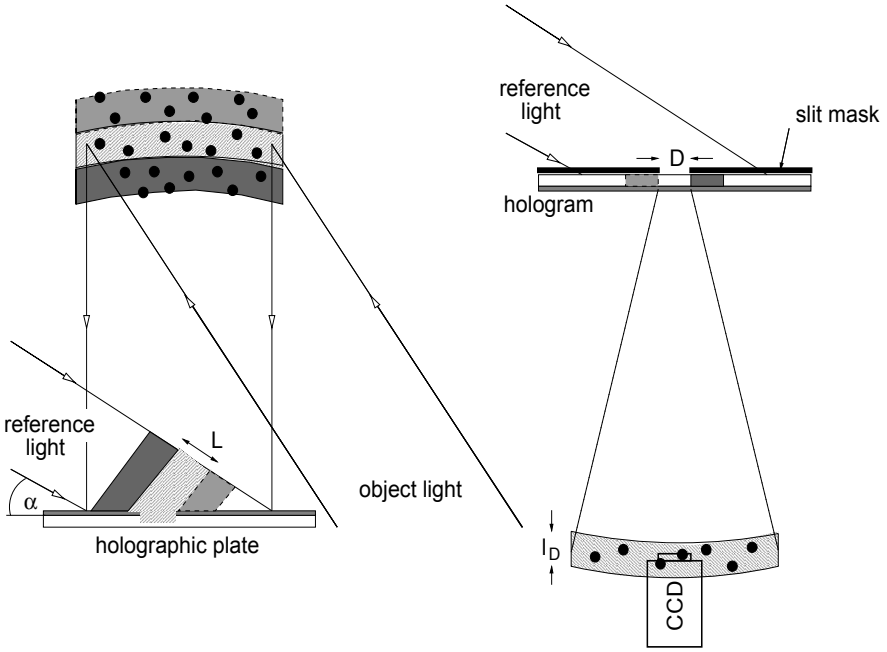

Fig. 2. Schematic of light-in-flight holography with short coherence length for particle recording (left) and reconstruction of real particle images (right).

1.4 Real particle images and their evaluation

For the reconstruction of a high fidelity real image a properly conjugated reference wave is needed in order to avoid distortions. Preferably light of the same wavelength is used to avoid cumbersome angular corrections. To serve as the conjugate wave in many setups a highly planar reference wave is used. It is essential that the propagation axis of this wave inclines again the same angle with the holographic plate after it has been exposed, developed and replaced – flipped, however, over its vertical axis. Alignment of such a setup can be critical especially when more than one reference beam is used for a double exposure recording (angular multiplexing for separable holograms and cross-correlation analysis) to determine the displacement of small particles with high accuracy (Sholes and Farell 2000). Furthermore, even small deviations from a planar wave (e.g. spherical aberrations from lenses) have an impact on the shape of particle images and their relative positions (Chan et al. 2000), which results in an artificial non-uniform displacement field superimposed on the original flow field.

The evaluation of holographic particle images is conducted by scanning the entire volume with a CCD sensor, either bare or in conjunction with a lens or microscope objective. This process is usually time consuming and strongly depends on the technical equipment used to translate the CCD and to acquire, pre-process and store the huge amount of image data from each single hologram. After or even during the acquisition these images are evaluated to extract the displacement data. Different setups to accomplish an effective but accurate evaluation have been presented in the past, based either on stereoscopic reconstruction for a larger aperture (Barnhart et

al. 1994), particle centroid extraction and correlation of their positions to reduce computing time and storage needs (Pu and Meng 2000) or combination of two perpendicular views (2D correlation as in ordinary PIV) to optimize the accuracy along the depth coordinate (Zhang 1997, Sheng et al. 2003). A straight-forward solution is the three-dimensional correlation of sub-image sets obtained by the scanning procedure. Due to the recent developments of computers this has become feasible and has been used in this study, yet in a preliminary and simple implementation.

A separated reconstruction setup can be favorable in HPIV for a couple of reasons, the most important being the possibility to operate it while a simple setup for recording can be used during the scanning and evaluation process of the previous recording. For measurements in costly wind tunnel facilities this helps to reduce their operating times significantly. Moreover, it can be avoided to reconstruct with pulsed laser sources, which are still expensive in operation and maintenance. Most of the flow recordings nowadays (either planar or three-dimensional) are obtained with Nd:YAG lasers, which are also available as continuous-wave lasers, yet in a compact design with reasonable output power and stable operation over some days. A stable operation of the reconstruction laser is one of the key-issues for high accuracy measurements and difficult to guarantee in high energy pulsed lasers. Slight deviations in the propagation direction of the reference beam caused by pulse-to-pulse variations are difficult to avoid when the laser has to be fired continuously during the scanning process. Whereas deviations during the recording can be corrected for by an appropriate system which records fixed calibration points in space in each hologram, a fact which has not yet been considered, probably due to an increasing complexity of both, the recording and reconstruction setup. Finally, in a separated setup with complex delivery of two reference beams the reconstructing and recording beams can be aligned independently.

2. Nd:YAG based measurement system for wind tunnel flows

In the present study the LiFH-technique was applied for the first time using a double cavity pulsed Nd:YAG laser ($\lambda = 532$ nm), especially designed for holographic flow measurements. A continuous wave Nd:YAG laser has then been used to build a separate setup allowing for intensity-integrated reconstruction of weak particle images from two superimposed light-in-flight holograms of a globally seeded wind tunnel flow.

2.1 Double cavity laser system for holographic flow analysis

For the study of wind tunnel flows a newly developed Nd:YAG laser system consisting of two laser heads and an external beam combination was used. The beams, produced from two Spectra Physics Quanta Ray Pro lasers are overlapped by a dichroic mirror to ensure maximum output power of each laser. Therefore, both beams are passing an external crystal for frequency-doubling, which only affects the 1064 nm-radiation. The beams are cross-polarized and have a nearly top-hat profile for a more homogenous illumination of the particle field. The maximum pulse energy is about 1.5 J at 10 Hz repetition rate for each laser. A nice feature of this system is a common laser seeder which allowed to choose between multi-mode operation for LiFH with a coherence length of some 7 mm and single mode operation for ordinary holography, where the coherence length is limited by the pulse width (typically some 7 ns). Thus a direct comparison was possible to show the advantages of this technique (Hinsch and Herrmann 2003).

2.2 Recording setup at the wind tunnel

In figure 3 the optical setup at the wind tunnel is shown true to scale. The open test section is about two meters wide and one meter deep. In the flow a generic airfoil produced two counter-rotating tip-vortices. A reference signal is produced by the first reflection from a glass wedge plate that is split into two polarization dependent reference beams by a polarizing beam splitter (TFP). A detailed side view showing both arms above and underneath the tunnel outlet is given in figure 4. A prism was mounted on a mechanical translation stage to control the path length of each reference beam. Since the coherence length L of the unseeded laser is some 7 mm, the path lengths need to be identical within 1 mm compared to the path length of the object beam. This travels over three bending mirrors (HEM) before it is expanded by a set of two coated lenses to illuminate a small part of the wake flow behind the profile. The position of the center of the measurement volume is located at a distance of some 35 cm from the holographic plate, which was placed exactly at the flow boundary – far enough to avoid vibrations affecting the stability of the measurement system, but close enough to ensure high signals from the scattering particles. The delivery of the reference beams was realized in a vertical arrangement in order to maintain the same azimuthal angle α of incidence onto the holographic plate, while the two recordings are distinguished by their height-angles $\pm\beta$.

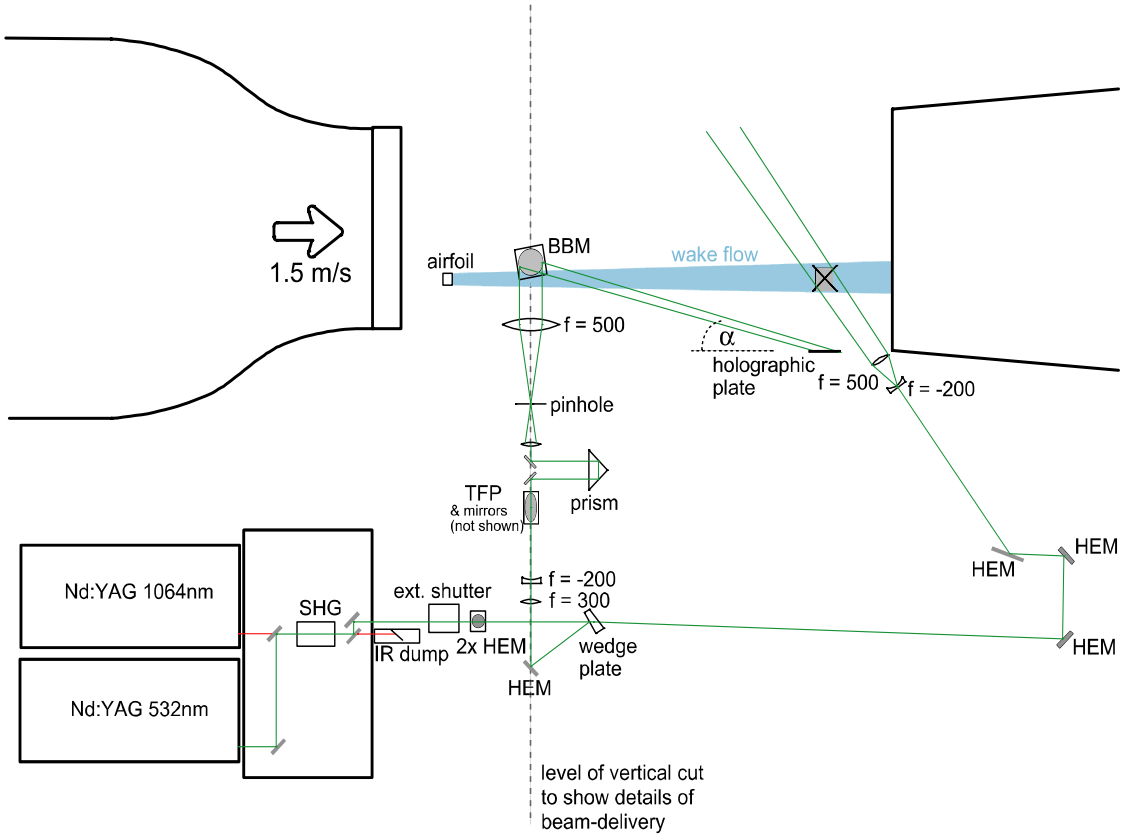

Fig. 3. Setup for recording LiFH-PIV holograms at the 1m wind tunnel at the German aerospace agency (DLR) in Goettingen, showing the beam paths from the laser heads through the combining optics and shutter, two mirrors (HEM) for adaption of the beam height to fit the measurement area and the optics for holography as explained in the text. For the out-of-plane propagation as indicated by the dashed line and details of the reference beams see Fig. 4.

Mind that the azimuthal-angle α determines the path difference along the plate. To reconstruct the same depth from two superimposed holograms it is thus necessary to direct the beams out of the plane to be incident on the plate under the same angle α but with a difference in the height-angle β.

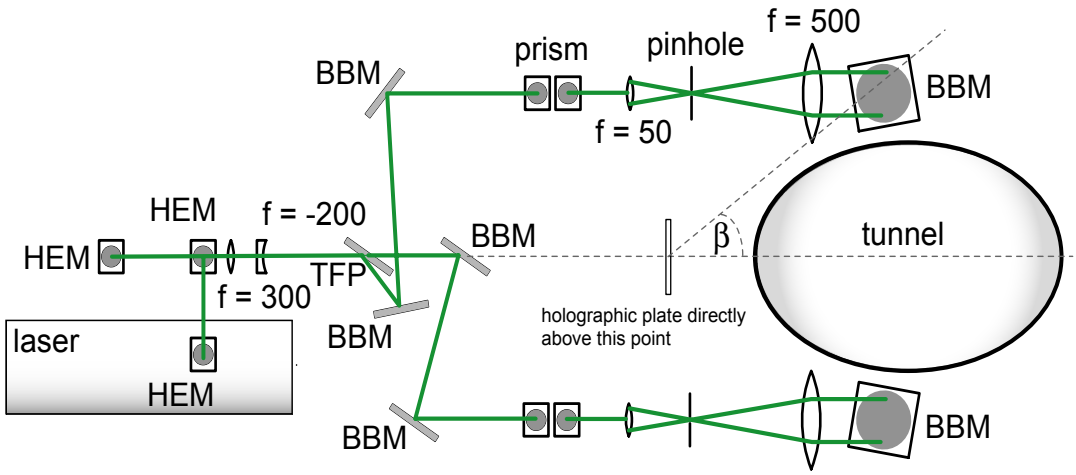

Fig. 4. Side view of the reference beams with spatial filters (pinhole) for a more uniform illumination of the holographic plate. Given in gray are the outlet of the wind tunnel and the cover box of the combining optics. The thin-film polarizer (TFP) directs each pulse according to its polarization into one of the optical arms, guided by specially coated broad-band-mirrors (BBM). The beam is then directed out of the projected plane towards the holographic plate.

Perfect collimation of the reference beams was controlled by a shearing interferometer. The beam profiles of the two laser heads showed intensity variations typical of a multi-mode laser which are changing with increasing distance from the laser-head aperture. Since a low pulse energy in the reference beams is already sufficient for a proper plate exposure, pinholes could be introduced without damages to improve the beam profile. A couple of holograms have been recorded under different conditions regarding type and size of particles as well as density – all having in common a very low amount of object light as compared to the reference light intensities. The mean flow of about 1,5 m/s produced rather stable vortices, but with fluctuating positions. Since there was no control to trigger the events, it turned out to be difficult to catch single vortices by the holographic method.

2.3 Separated reconstruction setup

To reconstruct particle image fields from the wind-tunnel-flow holograms – recorded under LiFH conditions – and extract image data throughout the whole volume an automatic read-out setup was developed. It comprises of the optical setup, two shutters, two mechanical translation stages and a controlling and image-acquisition unit based on a single PC with large storage capacities, a frame-grabber and a CCD camera module. In the following some details of this setup are described.

For this off-site reconstruction a continuous wave laser (Nd:YAG at $\lambda = 532$ nm with 150 mW in single longitudinal mode) with Gaussian beam profile is used. A top view of the beam handling unit (lower part of the setup) is shown in figure 5. Both the reference beams are expanded,

collimated and directed out of the plane by two highly planar (< λ/20) mirrors to illuminate the holograms. The collimation is checked by shearing plate interferometer. The relative positions of hologram and mirrors are precisely scaled down from the arrangement at the wind tunnel to produce the same angles of incidence as before. Above this beam-handling unit, the scanning unit is placed next to the holographic plate (figure 6, left, showing a vertical cut as indicated in figure 5). For the sake of convenience, the complete arrangement has been turned by 90° with respect to the original recording orientation and the illumination of the plate (figure 6, right) is from below. Thus, angle β is now the originally vertical component of the angle of incidence while the originally azimuthal component α determines the out-of-plane propagation direction in figure 5. Both the mechanical shutters, controlled by the computer, are used to block either reference beam.

Figure 6 indicates also the areas exposed by the two recording reference waves in gray shade, i.e., the contours of the holograms. They are elliptical because of the oblique incidence of the circular beams and they do not coincide because of their different height-angles ±β. The exact alignment of both beams is done by adjusting the mirrors with micro-screws under visual inspection of a calibration hologram recorded under the same conditions.

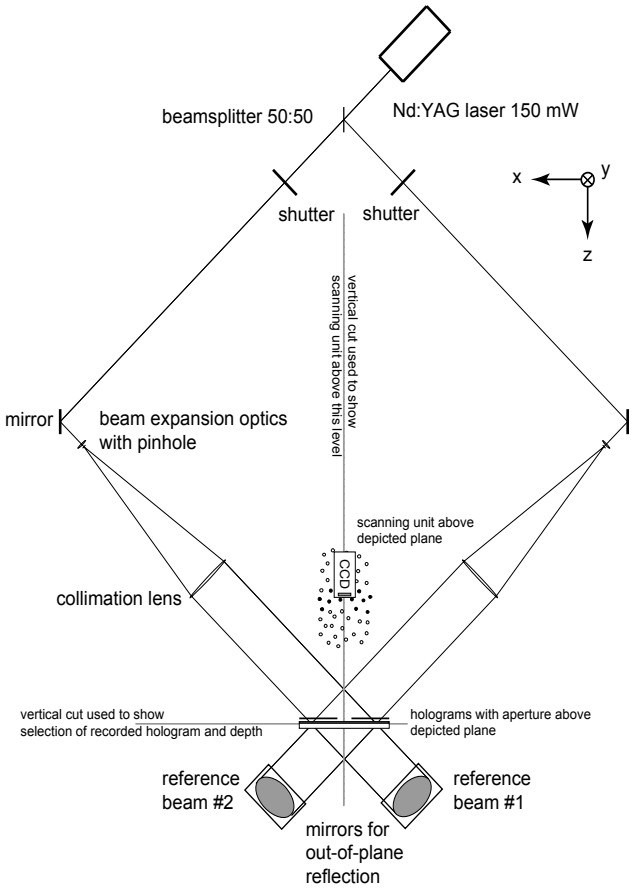

Fig. 5. Beam handling unit of the reconstruction setup for extracting real particle image fields from wind-tunnel recordings. Carefully collimated beams are propagating out of the plane to illuminate the holograms placed above, while the reconstructed real-image can be scanned by a CCD sensor.

During reconstruction, a circular aperture is moving along the bisector of the "propagation axes" (the tracks of the plane of incidence of the reference beams on the hologram) to select the region of depth currently under investigation. This aperture can be moved by a translation stage along the x- and y-direction. Another translation stage – in this case three-dimensional – controls the camera position as shown in the left part of figure 6. Both translation stages as well as the image acquisition and the exposure times of the CCD sensor are controlled by the PC.

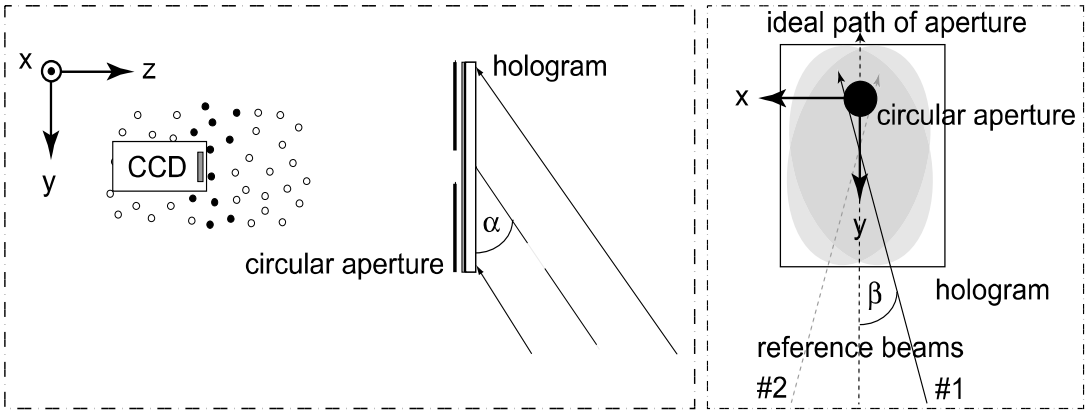

Fig. 6. Upper part of the reconstruction setup, showing the scanning unit (left) and the beam propagation towards the holograms (right). A moving aperture is used to select the corresponding depth according to the position of the sensor, while the beams are switched to reconstruct either particle field.

At each position of the sensor the reference beams are used alternately (switched by the mechanical shutters) to acquire both the successive images without moving the sensor. This avoids that a repositioning error can enter into the displacement measurement. A typical scanning process is started for a given xy-coordinate of the CCD-sensor. The sensor is then scanned along the z-direction while the position of the circular aperture on the hologram (setting the depth region) is following to provide reconstruction of the corresponding depth position. After a scan over the full depth is finished the same procedure is repeated for another xy-coordinate. Providing perfect alignment, a single aperture position should allow reconstruction of the same depth slice for both reference beams. Unfortunately, we have not yet succeeded in achieving the ideally aligned setup. This became evident when comparing both the reconstructed slices. Thus, a relationship between aperture position and reconstructed volume element was established empirically to control aperture positions for each hologram at a given sensor position throughout the whole scanning process.

It was already mentioned that a long-time exposure of the CCD sensor is used to compensate for low diffraction efficiencies of the particle holograms. This procedure was necessary for all evaluations of the flow holograms from wind tunnel experiments as exposure times usually used in CCD sensors (typically $\tau = 100\ \mu s$) turned out to be insufficient for proper image quality. By carefully minimizing all scattered light reaching the sensor from directions other than the hologram it was indeed possible to extract long-exposure (up to $\tau = 2$ s) particle images with a good signal-to-noise ratio. Scanning times, of course, have been increased drastically – yet it becomes possible to record volumes of sufficiently larger cross-sectional size.

The digital images are stored on a hard-disc drive, each identified by its position in space and the according reference beam. For their evaluation a three-dimensional gray-value correlation is

performed. A first version of a data handling routine has been implemented in Matlab®, assembling sub-volumes from the image data and carrying out the correlation by three-dimensional FFTs. The demand on memory and computing power is still enormous and should be relaxed by further refinements. The present procedure represents a straightforward solution to provide input data for extended common PIV algorithms. It should be mentioned that the current version is still a very simple implementation examining the correlation results by means of their maximum values and applying sub-pixel algorithms to extract more accurate displacement data. It is still due to refine this approach using evaluation techniques well known from PIV, like window-shifting, iterative steps and validation criteria, as well as filter and interpolation methods (Raffel et al. 1995).

3. Results

All holograms recorded at the wind tunnel have been examined in a first step as to their particle image quality and density. In an intermediate check during the measurement-campaign it turned out, that appropriate particle image densities are only obtained by very long operating times of the seeding-generator. To obtain a sufficient number of larger particles the generator was operated with lower pressure settings – that achieve a broader particle size distribution than commonly used in wind tunnel measurements – for up to one hour. According to previous measurements of size distributions about 50% of the particles were smaller than 1 μm and only 7.5% reached sizes larger than 3 μm.

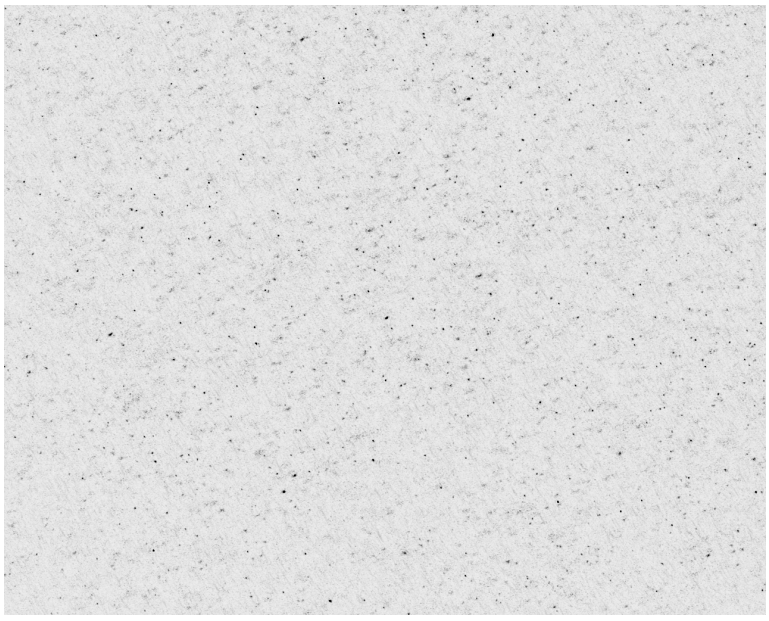

Fig. 7. Inverted image of a digitized plane (1280 px × 1024 px) from a reconstructed real image of a wind tunnel flow (DEHS particles after one hour of operation of the seeding generator). The image was obtained by an exposure time of 0,5 seconds, the field of view is 8,6 × 6,9 mm^2.

With a cross-sectional dimension of the object light beam of about 4 cm the scattered light intensities have thus been rather low. Judging from the type of reconstructed images we assume that only larger particles (i.e. $d_p > 1$ μm) contribute to the signals obtained from long-exposure reconstructions. Unfortunately, in most cases the particle image densities have still been too low

to allow for a proper correlation analysis on the images obtained. For the best hologram the particle density is high enough to evaluate the complete set of images by three-dimensional cross-correlations on 128^3 px-sub-volumes. Thus, a volume of $24{,}0 \times 18{,}8 \times 29{,}1$ mm^3 was scanned within 35 hours of operation time of the read-out-unit, the bottleneck still being the slow translation stage moving the circular aperture over the hologram between exposures.

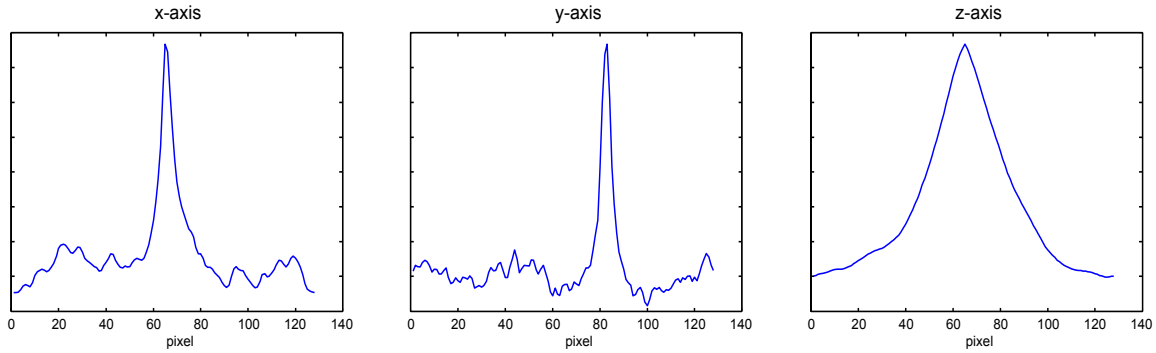

Fig. 8. Example profiles through the maximum value of a three-dimensional matrix of the correlation coefficient, the voxel size is 128×128×128 px^3 and corresponds to a size of the interrogation volume of $857 \times 857 \times 6272$ µm^3 , since the pixel-pitch in z-direction is 49 µm and in x,y-direction given by the pixel size of the CCD array (6,7 µm).

The result are 5409 image pairs, each 2,5 MB in size – in total more than 13 GB of image data. A sample plane from the reconstructed image is shown in figure 7. The noise level is still very low, allowing for a much higher number density of particle images within each single plane, yet their number was sufficient for a correlation analysis. Despite the maximum depth resolution (9,8 µm) of the translation stage, adjacent image planes have been acquired with a separation of 49 µm to facilitate the use of sub-pixel algorithms and to prevent from over-sampling the elongated particle images, a consequence of the small aperture used to determine the depth position of the reconstructed shell within the measurement volume. Thus, the resulting interrogation volumes are $857 \times 857 \times 6272$ µm^3 in size.

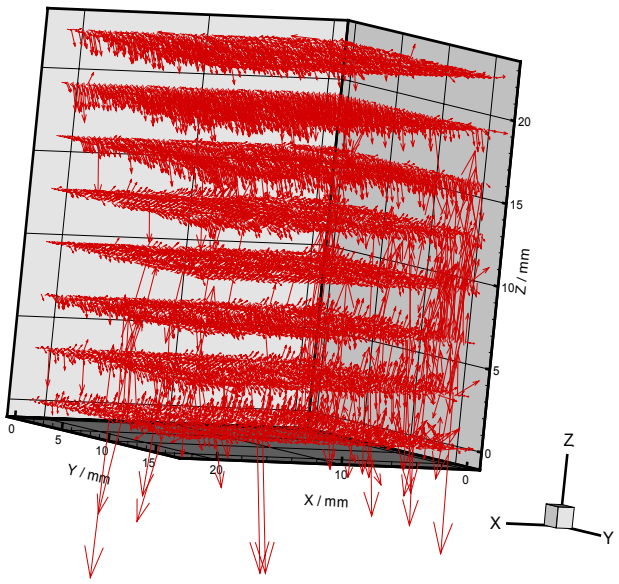

Fig. 9. Evaluated wind tunnel flow, 16.640 vectors have been obtained by three-dimensional gray-value correlation. The plane-like distribution of the vectors is a result of a relatively large separation between adjacent image slices, from which 128 enter in each correlation.

In figure 8 three cuts through the maximum value in a matrix of correlation coefficients are shown. Along the x- and y-direction the correlation function is similar to those known from two-dimensional PIV, while along the z-direction a much broader peak is observed.

As mentioned before, the moving vortices behind the generic air-foil provided an unfavorable flow configuration. A single snap-shot hologram of a small region is unlikely to reveal characteristic parts of a single vortex. Therefore, it is not astonishing that the hologram yields mainly the mean velocity of the wind-tunnel flow, which was parallel to the y-direction. Figure 9 shows the complete correlation result, a total of 16.640 vectors have been obtained from an evaluation with 50% overlap of the interrogation cells (IC) in each direction. The plane-like distribution is a result of the densely-spaced grid points along the x- and y-direction and the much wider spacing (approx. $\times$ 7,3) along the z-direction. Besides some spurious vectors due to poor image quality in the lower part a net flow perpendicular to the mean flow is observed in some regions producing the arrows that project out of the planes (e.g. upper part). Since the mean flow is not clearly visible in this representation a detailed view of the velocities in the interior of the flow field is shown in figure 10, the corresponding correlation coefficients are given as a countour plot in one plane. Here, an overlap of 75% was used, increasing the total number of vectors to 124.800 within the same volume. Even if these results do not furnish important flow data, it was shown that particle images could be extracted, of a quality sufficient for further processing – yet with still too low a particle density. A maximum depth of 47 mm has been covered from other holograms, the useable cross-section of the measurement volume extended to 30×30 mm^2 providing particles of sufficient brightness even at its border.

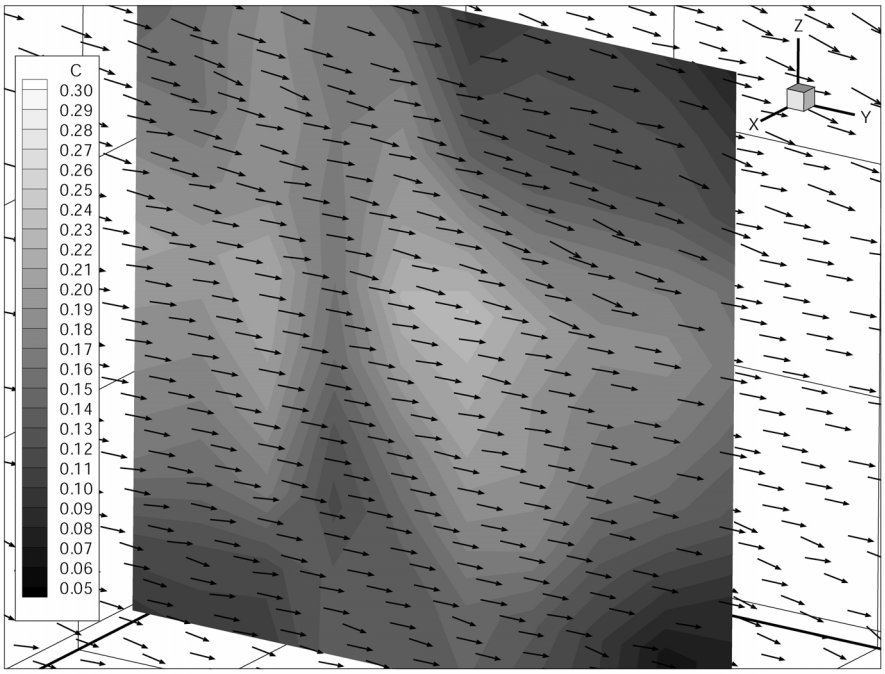

Fig.10. Detailed view, from inner part of the evaluated volume, showing the three-dimensional velocity distribution and the correlation-coefficient (C) in one slice as a measure for the reliability of the velocity value.

4. Conclusion and outlook

It has been demonstrated that a special version of HPIV – the so-called LiFH-PIV which facilitates effective background noise reduction by use of a short coherence light source for the recording – is capable of mapping the three-dimensional flow field from a globally seeded large wind tunnel flow. The utilization of a separate reconstruction setup using a continuous wave laser effectively reduces the operating time of the wind tunnel and allows for simultaneous evaluation procedures. Furthermore, low intensity particle images have been analyzed by an integrating reconstruction method, thus reducing the effective energy density of the pulsed illumination light needed for the recording and allowing for considerably larger cross-sections of the measurement volume. For the first time a three-dimensional gray value correlation of sub-volumes to analyze an extended volume mapped by particle holography has been reported. This approach, yet very time consuming and with high demands on computer power, is favorable when advanced evaluation algorithms are envisaged, from most of which can be extended without loss of generality from the two-dimensional case. The restricted depth resolution, one of the drawbacks of LiFH-PIV, however, needs to be addressed in further refinements of this technique. Reconstructions with larger effective apertures are feasible without impairing the principle of limited depth reconstruction. For further wind tunnel measurements the production of seeding particles needs to be optimized in terms of size distribution and density. For this purpose, investigations have been made to understand the physical processes of particle generation (Kaehler et al. 2002) and the influence of particle parameters on the holographic imaging process (Pu et al. 2002). Increasing seeding densities could allow for smaller ICs, with 64 px or even 32 px side-length and also non cubic ICs in the pixel-domain are feasible.

Acknowledgement

The support of the wind tunnel measurements from the team at DLR in Göttingen, Germany is greatly acknowledged. The authors would like to thank J. Agocs, H. Frahnert, J. Kompenhans, B. Sammler and A. Schröder personally for their help during the campaign.

This work has been performed under the EUROPIV2 project. EUROPIV2 (A joint program to improve PIV performance for industry and research) is a collaboration between LML URA CNRS 1441, DASSAULT, AVIATION, DASA, ITAP, CIRA, DLR, ISL, NLR, ONERA and the universities of Delft, Madrid, Oldenburg, Rome, Rouen (CORIA URA CNRS 230), St Etienne (TSI URA CNRS 842), Zaragoza. The project is managed by LML URA CNRS 1441 and is funded by the European Union within the 5th frame work (Contract N°: G4RD-CT-2000-00190).

References

Abramson N (1996) Light-in-flight or the holodiagram: the columbi egg of optics. SPIE Optical Engineering Press, Bellingham, Wash

Barnhart DH, Adrian RJ Papen GC (1994) Phase-conjugate holographic system for high-resolution particle image velocimetry. Appl. Opt. 33: 7159-7170

Bjelkhagen HI (1995) Silver-halide recording materials for holography and their processing. Springer-Verlag, Berlin

Bohren CF and Huffman DR (1983) Absorption and scattering of light by small particles. Wiley Science, New York

Chan KT, So RMC, Wong WO, Li YJ (2000) Particle image aberrations in off-axis holography. In: Carlomagno GM, Grant I (eds) 9th Int. Symp. on Flow Visualization, Edinburgh

Geiger M, Herrmann SF, Hinsch KD, Peinke J (2000) Analysis of free jet turbulence with cross-correlation light-in-flight holography (LiFH). Proc. Euromech 411, Rouen

Goodman JW (1967) Film grain noise in wavefront-reconstruction imaging, J. Opt. Soc. Am. 57.4: 493-502

Herrmann SF, Hinsch KD (2001) Particle holography and the noise limit. In: Kompenhans J (ed) 4th Int Symp on Particle Image Velocimetry, DLR-Mitteilung 2001-03, Göttingen

Hinrichs H, Hinsch KD, Kickstein J, Böhmer M (1997) Light-in-flight holography for visualization and velocimetry in three-dimensional flows. Opt. Lett. 22: 828-830

Hinrichs H, Hinsch KD, Netter R, Surmann C (1998) Light-in-flight particle holography for velocimetry in a wind tunnel. In: Carlomagno GM, Grant I (eds) 8th Int. Symp. on Flow Visualization, Sorronto, pp 19.1-19.5

Hinsch KD (2002) Holographic particle image velocimetry. review article Meas Sci Technol 13: R61-R72

Hinsch KD and Herrmann SF (2003) Signal quality improvements by short-coherence holographic particle image velocimetry. Proc. Int. Workshop on Holographic Metrology in Fluid Mechanics, Loughborough

Kähler CJ, Sammler B, Kompenhans J (2002) Generation and control of tracer particles for optical flow investigations in air. Exp. Fluids 33:736-742

Kozma A (1968) Effects of film-grain noise in holography, J. Opt. Soc. Am 58:436-438

Pu Y and Meng H (2000) An advanced off-axis holographic particle image velocimetry (HPIV) system. Exp. Fluids: S117-28

Pu Y, Cao L, Meng H (2002) Fundamental issues and latest development in holographic particle image velocimetry. International Mechanical Engineering Congress & Exhibition , Paper 33171, ASME, New Orleans

Raffel M, Willert C, Kompenhans J (1998) Particle image velocimetry – a practical guide. Springer Verlag, Berlin

Sheng J, Malkiel E, Katz J. (2003) Single beam two-views holographic particle image velocimetry. Appl. Opt IP 42.2: 235 to appear

Sholes K, Farrell PV (2000) Optical alignment-induced errors in holographic particle image velocimetry. Appl. Opt. vol 39 31:5685-5693

Zhang J. Tao B, Katz J (1997) Turbulent flow measurement in a square duct with hybride holographic PIV. Exp Fluids 23: 373-381